Immunity 24, 475–487, April 2006 ©2006 Elsevier Inc. DOI 10.1016/j.immuni.2006.02.008

Induction of a Homeostatic Circuit in Lung Tissue by Microbial Compounds

Kenji Takabayshi,[1] Maripat Corr,[1] Tomoko Hayashi,[1] Vanessa Redecke,[1] Lucinda Beck,[1] Donald Guiney,[1] Dean Sheppard,[2] and Eyal Raz[1,*]

[1] Department of Medicine
University of California, San Diego
La Jolla, California 92093

[2] Lung Biology Center
University of California, San Francisco
San Francisco, California 94158

Summary

TGFβ presented and activated by integrin αvβ6 expressed on alveolar epithelial cells (AEC) continuously inhibits the functionality of alveolar macrophages (AM). Despite this inhibition, AM retain their ability to respond to inhaled microorganisms. Herein we describe a homeostatic circuit through which the effects of microbial products on macrophages transiently circumvent this inhibition by repressing αvβ6 expression on AEC. Subsequent production of matrix metalloproteinases by activated AM activates latent TGFβ, reinduces αvβ6 expression, and thereby reinstates tonic inhibition of AM function. Our results reveal how AM can be activated while minimizing their potential to inflict collateral damage to the adjacent lung tissue and indicate that tissue-specific microenvironmental factors shape organ-specific defensive strategies against microbial invasion.

Introduction

Previous investigations have documented an immunosuppressive microenvironment within the normal lung (Bingisser and Holt, 2001; Munger et al., 1999). Indeed, different studies have indicated that AM are inefficient in providing accessory cell-like activity compared to macrophages from other tissues. In fact, AM have been shown to suppress dendritic and T and B cell functions most likely by the secretion of NO, PGE2, IL-10, or TGFβ (Lipscomb et al., 1993; Thepen et al., 1994).

TGFβ is a pleiotropic cytokine that modulates a variety of biological processes such as cell growth, apoptosis, extracellular matrix synthesis, inflammation, and immune responses (Fitzpatrick and Bielefeldt-Ohmann, 1999; Shi and Massague, 2003). Mature TGFβ is secreted in a complex with its N-terminal fragment, the latency-associated peptide (LAP), which inhibits its function. Latent TGFβ is activated extracellularly by proteolytic cleavage or by interaction with thrombospondin or with specific integrins including αvβ6 (Annes et al., 2003).

Integrins are dimeric cell-surface receptors composed of α and β subunits (Hynes, 2002; van der Flier and Sonnenberg, 2001). A recent study has demonstrated that the epithelial integrin, αvβ6, binds to TGFβ LAP and activates TGFβ (Munger et al., 1999). Subsequently, the activated TGFβ binds to its receptors on AM or fibroblasts and leads to the cytostatic suppression of AM functionality. Mice lacking the αvβ6 integrin have spontaneously activated AM, and reexpression of the integrin in a subset of alveolar epithelial cells suppresses this macrophage activation (Morris et al., 2003).

The respiratory tract is exposed constantly to inhaled particles and microorganisms that are usually cleared by a coordinated movement of the mucociliary epithelium in the upper airways and by AM in the alveolar space. As the major sentinel of innate immunity in the alveolar space, AM should be capable of responding appropriately to inhaled microorganisms. The mechanism by which AM perform this task in the presence of continuous and tonic inhibition by TGFβ is still unclear. Our results presented below describe a homeostatic circuit in which microbial compounds initiate and then suppress AM activity via complex interactions with AEC involving the regulation of integrin αvβ6 expression.

Results

TLR Ligands Suppress Integrin αvβ6 Expression in the Lung

The family of Toll-like receptors (TLR) is one of the main microbial sensing systems of innate immunity (Krutzik and Modlin, 2004; Takeda et al., 2003). By interacting with a variety of signature microbial compounds, TLR initiate inflammatory and protective responses in the host. To evaluate the effect of TLR ligands on the expression of integrin αvβ6, we initially injected an immunostimulatory oligonucleotide (ISS-ODN, also known as CpG-ODN, a TLR9 ligand) i.v. into C57Bl/6 mice. The lungs were harvested, and the kinetics of mRNA and protein expression of integrin αv and β6 subunits was analyzed. While the mRNA levels of TGFβ1 were unchanged, those of integrin αv and β6 subunits were profoundly diminished as measured by RT-PCR (Figure 1A) as well as concordant protein levels as measured by immunoblot (Figure 1B). Next, to confirm that this gene suppression of integrin αv and β6 is not restricted to ISS-ODN, other TLR ligands were also tested. All other TLR ligands tested showed a similar profile (Figure 1C), demonstrating that this phenomenon applies to at least those TLR ligands tested. In initial experiments, ISS-ODN was i.v. injected into mice; however, in reality TLR ligands enter the lung from the outside environment. To simulate by a more natural route, ISS-ODN was intratracheally (i.t.) administered, and this i.t. administration resulted in the same inhibition of integrin αvβ6 (Figure 1D).

Despite i.v. administration of ISS-ODN that systemically distributed the compound throughout the entire body, the inhibition of integrin αvβ6 was a lung-specific event, as other organs analyzed did not display this inhibitory effect (Figure 1E).

*Correspondence: eraz@ucsd.edu

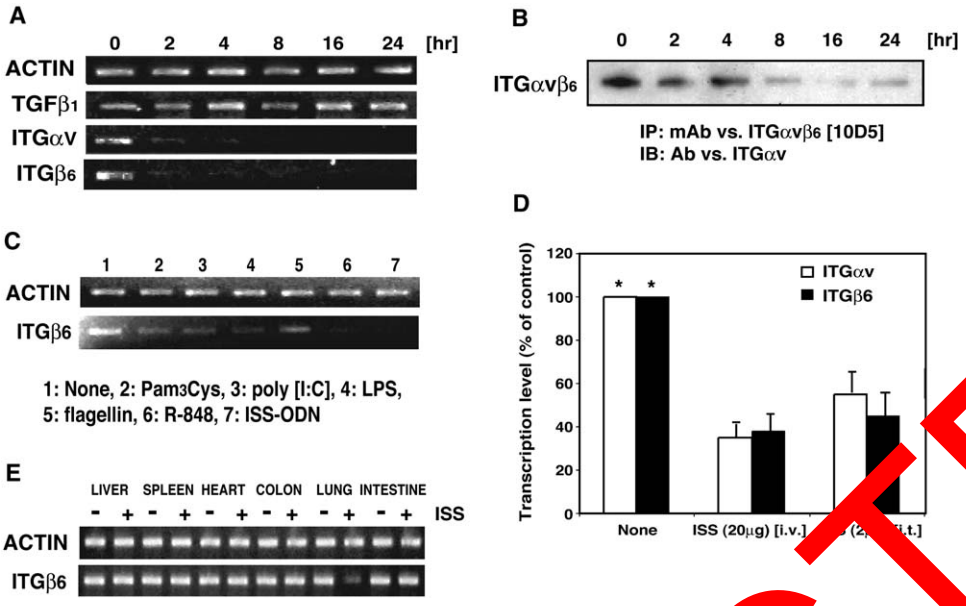

Figure 1. TLR Ligands Suppress Integrin αvβ6 Expression in the Lung Tissue

(A) ISS-ODN (TLR9 ligand) suppresses the transcript levels of integrin αvβ6 in lung tissue. ISS-ODN (20 μg/mouse) was i.v. injected into C57Bl/6 (B6) mice. Transcript levels of TGFβ1, integrin αv (ITGαv), and integrin β6 (ITGβ6) were analyzed by RT-PCR.

(B) ISS-ODN inhibits protein expression of integrin αvβ6 in lung tissue. B6 mice were i.v. injected with ISS-ODN (20 μg/mouse) and lung tissue homogenates were prepared. The integrin αvβ6 was immunoprecipitated with anti-β6 monoclonal Ab (10D5) and then immunoblotted with anti-integrin αv polyclonal abs.

(C) Different TLR ligands suppress the transcription of integrin β6 in lung tissue. B6 mice were i.v injected with the following TLR ligands: Pam3Cys (50 μg, TLR2), poly (I:C) (50 μg, TLR3), LPS (10 μg, TLR4), flagellin (50 μg, TLR5), or R848 (20 μg, TLR7). The transcript levels of integrin β6 (ITGβ6) in lung tissue were analyzed by RT-PCR 24 hr later.

(D) Comparison of intratracheal (i.t.) to i.v. injection. ISS-ODN was administered into B6 mice via i.v. injection (20 μg/mouse) or i.t. instillation (2 μg/mouse). The mRNA levels of integrin β6 (ITGβ6) and integrin αv (ITGαv) in lung tissue were analyzed by qPCR 24 hr later. *p < 0.02 between ISS-injected to noninjected groups.

(E) Tissue-specific suppression of integrin β6 by ISS-ODN. B6 mice were i.v. injected with ISS-ODN (20 μg/mouse). The transcript levels of integrin β6 in the various tissues were analyzed by RT-PCR.

The data are shown as the mean ± SD and are representative of two or more experiments.

Suppression of Integrin αvβ6 Expression Is Linked to Downregulation of TGFβ Signaling

The genetic deletion of integrin β6 results in a defect in TGFβ activation and the consequent activation of AM (Morris et al., 2003). If integrin αvβ6 is in fact a key activator of latent TGFβ in the lung, suppression of integrin αvβ6 should lead to the downregulation of the basal phosphorylated levels of Smad2/3. Thus, we hypothesized that the administration of TLR ligands might also inhibit TGFβ signaling. Indeed, the levels of pSmad2/3 were reduced in lung lysates and in AM (Figure 2A) after ISS-ODN administration. However, this effect of ISS-ODN administration was not observed in mice in which the human integrin β6 is continuously expressed in the lung tissue (Figure 2B).

In Vivo Administration of ISS-ODN Increases the Responsiveness of AM to LPS In Vitro

The data presented thus far suggested that after ISS-ODN administration, AM are released from TGFβ-mediated suppression. To test this prediction, we measured and compared the responsiveness of both AM and peritoneal macrophages (PM) isolated from naive mice and from mice pretreated with ISS-ODN to subsequent LPS (TLR4 ligand) stimulation in vitro. The transcript levels of TNFα and IL-6 were measured by qPCR. AM isolated from ISS-pretreated mice displayed higher levels of these transcripts than AM from naive mice, in contrast to PM that displayed a mRNA profile that is consistent with endotoxin tolerance (Figures 2C and 2D) (Dobrovolskaia et al., 2003). However, this effect of ISS-ODN pretreatment on subsequent LPS stimulation in vitro was not observed in mice in which the human integrin β6 is continuously expressed in the lung tissue (Figure 2E).

AM Initiate the Inhibition of Integrin αvβ Expression on AEC

We next explored the mechanisms by which TLR signaling suppressed the expression of integrin αvβ6 subunits by using bone marrow (BM) chimeric mice. In control irradiated wt recipient mice that were reconstituted with wt BM, administration of ISS-ODN successfully diminished the transcription level of integrin β6 compared to that observed for TLR9$^{-/-}$ recipients that received wt BM. In contrast, the administration of ISS-ODN failed to reduce integrin β6 levels in chimeric mice that had TLR9$^{-/-}$ BM in wt recipients and TLR9$^{-/-}$ BM in TLR9$^{-/-}$ recipients (Figure 3A). Additionally, in TLR9$^{-/-}$ mice that had their resident AM depleted by i.n. delivery of clodronate liposomes (resulting in a 70%–90% depletion of resident AM 48 hr after liposome delivery), only

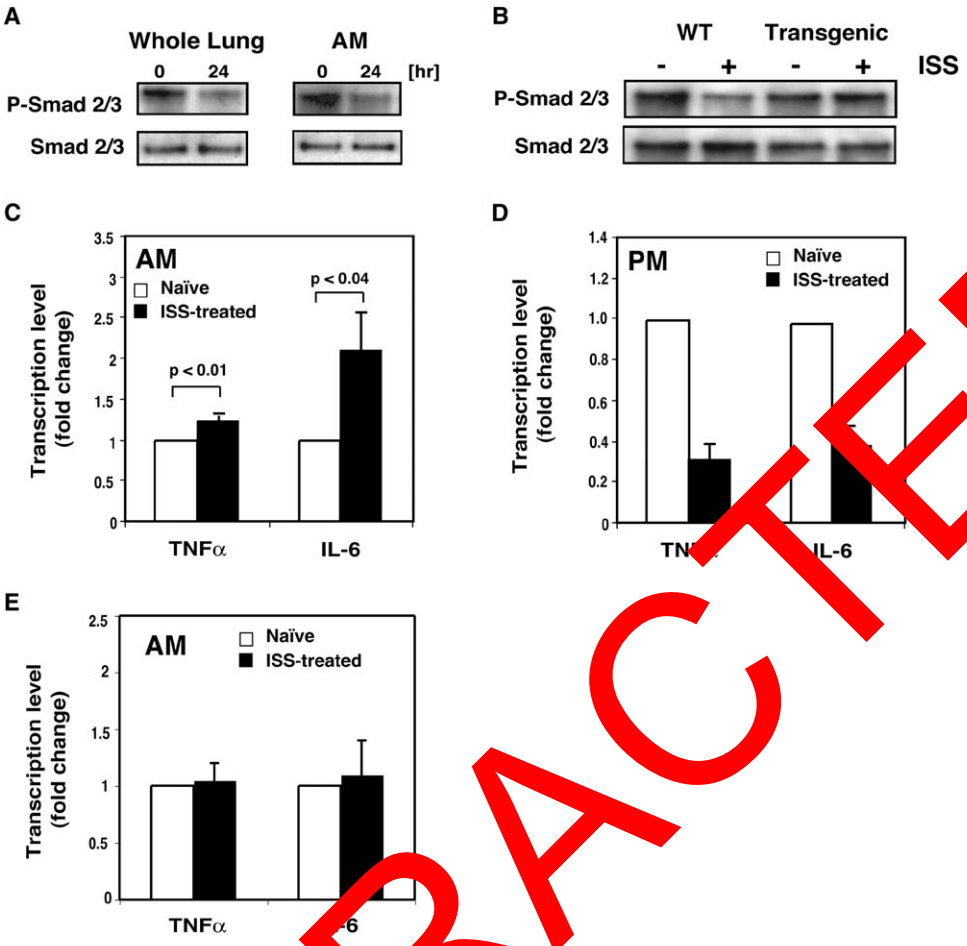

Figure 2. Suppression of Integrin αvβ6 Expression Is Linked to Downregulation of TGFβ Signaling

(A) ISS-ODN suppresses TGFβ signaling. Balb/c mice were i.v. injected with ISS-ODN (20 μg per mouse). At 24 hr postinjection, homogenates of lung tissue or of AM were prepared. Smad 2/3 was immunoprecipitated with anti-Smad 2/3 abs and then immunoblotted with anti-pSmad2/3 abs.

(B) ISS-ODN fails to suppress TGFβ signaling in hITGβ6 transgenic mice. Human ITGβ6 transgenic mice (B6) in which the human ITGβ6 gene is constitutively expressed under the human surfactant protein C promoter were i.v. injected with ISS-ODN (20 μg/mouse). At 24 hr postinjection, homogenates of lung tissue were prepared and the levels of pSmad2/3 were measured as described above.

(C and D) In vivo administration of ISS-ODN increases the responsiveness of AM (C) but not PM (D) to a subsequent in vitro LPS stimulation. AM and PM were isolated from naive or from ISS-injected mice (20 μg/mouse) 24 hr postinjection. The cells (2×10^5/well) were then stimulated with LPS (10 ng/ml) for 2 hr. The transcript levels of TNFα and IL-6 were analyzed by qPCR.

(E) In hITGβ6 transgenic mice, the injection of ISS-ODN fails to increase the responsiveness of AM to a subsequent in vitro LPS stimulation. AM were isolated from naive or ISS-injected hITGβ6 transgenic mice (20 μg/mouse) 24 hr postinjection. The cells (2×10^5/well) were then stimulated with LPS (10 ng/ml) for 2 hr. The transcript levels of TNFα and IL-6 were analyzed by qPCR.

The data are shown as the mean ± SD and are representative of two or more experiments.

Adoptively transferred wt AM and not TLR9$^{-/-}$ AM showed a reduction in integrin β6 transcription levels 2 hr after i.v. administration of ISS-ODN (Figure 3B). Furthermore, direct stimulation of an AEC line (MLE12) with ISS-ODN did not inhibit the expression of integrin αvβ6 (data not shown). Taken together, these results indicate that AM are the cells that respond to TLR ligands and initiate the subsequent inhibition of integrin αvβ6 expression on AEC (Figures 3A and 3B).

We then evaluated whether a soluble factor secreted by TLR9-activated hematopoietic cells inhibits integrin αvβ6 expression. We injected ISS-ODN to IFNα/βR$^{-/-}$, IFNγ$^{-/-}$, IL-10$^{-/-}$, COX2$^{-/-}$, IL-12p40$^{-/-}$, and TNFα$^{-/-}$ mice (i.e., TLR9-induced genes). As presented in Figure 3C, the administration of ISS-ODN to each of these mutant mice suppressed β6 transcript levels in the lung similar to wt mice. To further explore the potential contribution of other soluble factors secreted by TLR9-activated cells, we prepared conditioned medium (CM) from a single-cell suspension prepared from wild-type whole lung or spleen that was stimulated in vitro with ISS-ODN. The intraperitoneal (i.p.) injection of lung CM to wt and to TLR9-deficient mice failed to suppress the expression levels of integrin αvβ6, suggesting that a TLR9-induced soluble factor did not mediate the observed inhibition of integrin αvβ6 (Figure 3D). Similar results were obtained upon i.p. injection with spleen CM (data not shown). Although a role for a short-lived soluble mediator cannot be excluded and the specific hematopoietic cell(s) activated by TLR ligands are still unidentified, these results favor a cognate interaction between AM and AEC.

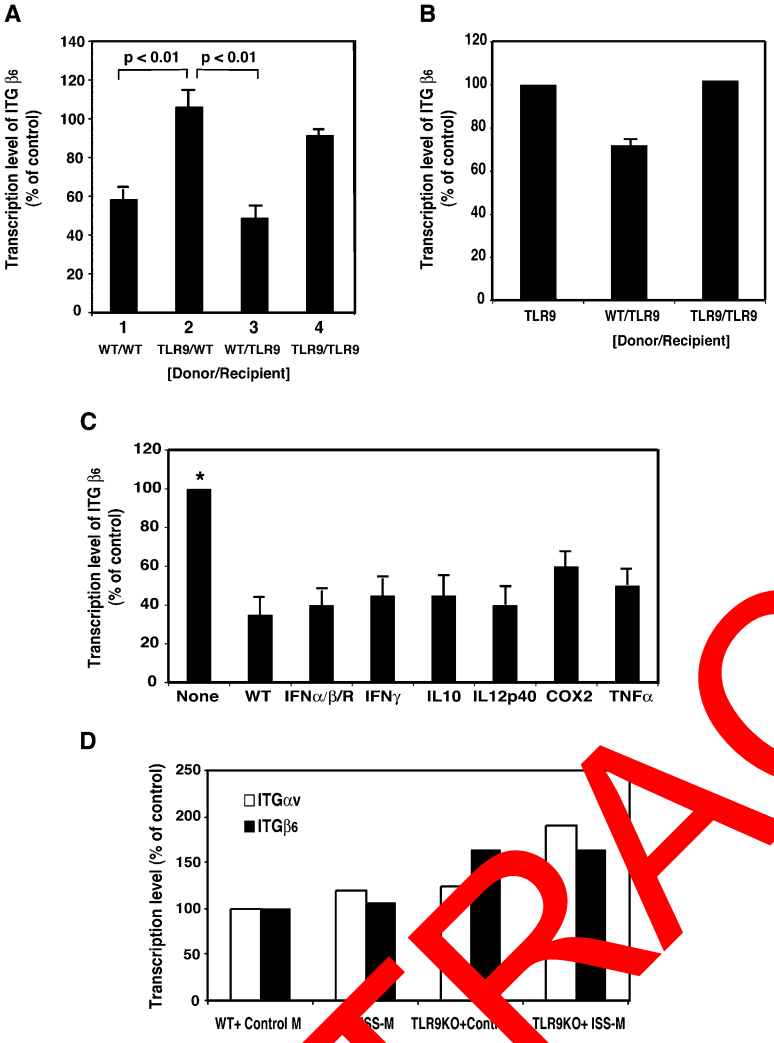

Figure 3. AM Initiate the Inhibition of Integrin αvβ6 Expression on AEC

(A) TLR9 in BM cells dictates the inhibition of integrin αvβ6 on AEC by ISS-ODN. Four sets of wt/TLR9 bone marrow (BM) chimeric mice were generated. Mice were injected i.v. with ISS-ODN (20 μg/mouse), the lung tissues were harvested 24 hr later, and the levels of integrin β6 were analyzed by qPCR in lung homogenates. Lane 1, wt recipients that received wt BM; lane 2, wt recipients that received TLR9$^{-/-}$ BM; lane 3, TLR9$^{-/-}$ recipients that received wt BM; lane 4, TLR9$^{-/-}$ recipients that received TLR9$^{-/-}$ BM.

(B) AM dictates the inhibition of integrin αvβ6 on AEC by ISS-ODN. Resident AM were depleted in TLR9$^{-/-}$ mice by clodronate liposomes delivered i.n. to the lung. AM were isolated from either wt or TLR9$^{-/-}$ mice and then intratracheally transferred (2×10^6 per mouse) to recipient TLR9$^{-/-}$ mice 48 hr after delivery of the liposomes. 24 hr later, mice were i.v. injected with 20 μg ISS-ODN. After another 24 hr, the lungs were harvested and levels of integrin β6 measured in lung homogenates by qPCR. The data represent one out of two experiments.

(C) TLR9-induced cytokines do not mediate the suppression of integrin β6 by ISS-ODN. ISS-ODN (20 μg/mouse) was i.v. injected to IFNγβR$^{-/-}$, IFNγ$^{-/-}$, IL12p40$^{-/-}$, TNFα$^{-/-}$, IL10$^{-/-}$, and COX2$^{-/-}$ mice. The transcript levels of integrin β6 in lung homogenates were analyzed by qPCR 24 hr later. *p < 0.02 between ISS-injected and noninjected groups.

(D) In vivo injection of conditioned medium prepared from lung cells treated with ISS-ODN failed to suppress gene transcription of integrin αvβ6. Conditioned media was prepared by treatment of a single cell suspension of lung tissue (B6 mice) with ISS-ODN (10 μg/ml) for 24 hr. Thereafter, conditioned media was intraperitoneally injected into B6 mice or TLR9$^{-/-}$ mice. The transcript levels of integrin αvβ6 in lung tissue were analyzed by qPCR 24 hr later.

The data are shown as the mean ± SD and are representative of two or more experiments.

TGFβ Is an Intermediary in the Cognate Interaction between AM and AEC

As TGFβ was previously proposed to induce integrin αvβ6 expression (Zambruno et al., 1995), we evaluated its regulatory role in our system. The incubation of two different AEC lines (MLE12 and MLE15) with active TGFβ resulted in the increase of gene expression levels of integrin αv, integrin β6, TβRI (TGFβ receptor I), and TβRII (TGFβ receptor II) (Figure 4A and data not shown for MLE15). Coculture of primary AM with the AEC line, MLE12, induced the expression of integrin β6 on AEC, and the administration of anti-TGFβ ab inhibited this induction (Figure 4B). The physical association between the AM and AEC was mandatory for this process since the coincubation of AM and AEC in a bichamber system that prevented cell-to-cell contact did not induce the expression of integrin β6 on AEC. To further identify the nature of the cognate interaction between AM and AEC that drives the expression of integrin β6 on AEC, we treated AM with anti-integrin αv ab prior to their coculture with AEC. The anti-integrin αv ab blocked the induction of integrin β6 on AEC (Figure 4B). Taken together, these data suggest that physical association between the AM and AEC enhances TGFβ production and that integrin αv expressed on AM with TGFβ are required to trigger integrin β6 expression on AEC.

To further establish the potential involvement of TGFβ in the regulation of integrin αvβ6 expression on AEC, active TGFβ was coinjected with ISS-ODN to wt mice. Indeed, the administration of active TGFβ blocked the suppression of integrin β6 transcription induced by ISS-ODN (Figure 4C) and inhibited the LPS-induced TNFα and IL-6 transcript levels in AM in vitro (Figure 4D). As TGFβ induces its own receptors (Figure 4A), the reduction in integrin αvβ6 levels on AEC (Figure 1A) is also expected to inhibit the expression of these

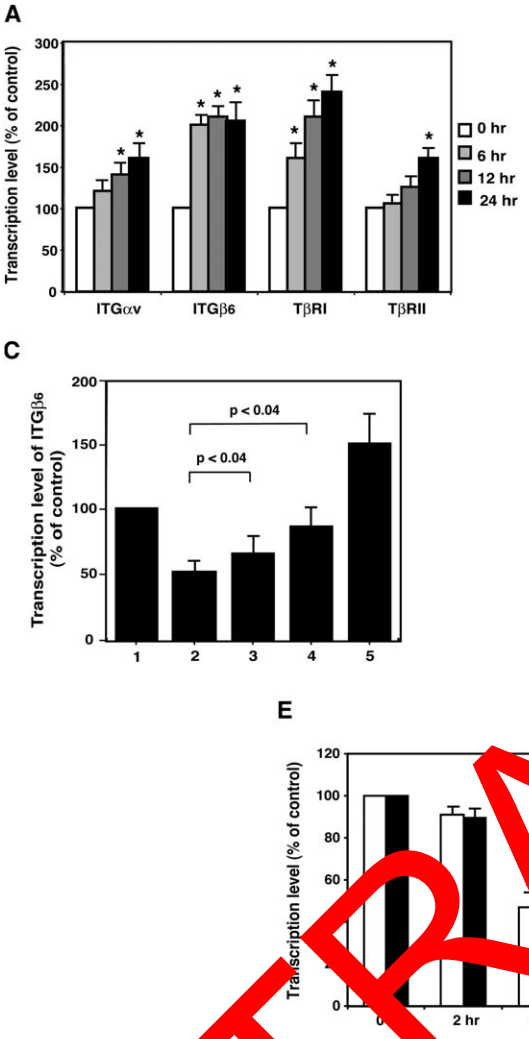

Figure 4. TGFβ Is an Intermediate in the Cognate Interaction between Primary Isolated AM and AEC

(A) TGFβ induces gene induction of integrin αv and β6 and TGF receptor-I and -II (TβRI and II). A mAEC line, MLE12, was incubated with 10 ng/ml of recombinant active TGFβ. AEC were harvested, and the transcription levels of integrin αv and β6 as well as TβRI and II were analyzed by qPCR as indicated. *p < 0.01 in comparison to the 0 hr levels in each group.

(B) Coculture of AEC with primary AM induces the expression of TGFβ-dependent ITGβ6 gene transcription. MLE12 was bi- or cocultured with AM in absence or presence of 10 μg/ml anti-TGFβ antibody. Lane 1, MLE12 alone; lane 2, MLE12 + AM (biculture); lane 3, MLE12 + AM (coculture); lane 4, MLE12 + AM (coculture) + anti-TGFβ ab; lane 5, MLE12 + AM (coculture) + anti-αv ab; lane 6, MLE12 + AM (coculture) + control ab. Similar results were obtained for the expression of TβRI and TβRII on AEC (data not shown).

(C) Exogenous TGFβ overcomes the suppression of ITGβ6 gene transcription caused by ISS-ODN in lung tissue. Active TGFβ was coinjected with ISS-ODN to B6 mice. Levels of integrin β6 were analyzed by qPCR 24 hr later. Lane 1, naive; lane 2, ISS-ODN (20 μg/mouse); lane 3, ISS-ODN with TGFβ (5 ng/mouse); lane 4, ISS-ODN with TGFβ (50 ng/mouse); lane 5, TGFβ (50 ng/mouse).

(D) Inhibition of active TGFβ blocks the increase in AM responsiveness to a subsequent in vitro LPS stimulation. Active TGFβ (50 ng/mouse) was coinjected with ISS-ODN (20 μg/mouse) to B6 mice. 24 hr postinjection, AM were stimulated with LPS (10 ng/ml) for 2 hr, and the transcript levels of TNFα and IL-6 were analyzed by qPCR.

(E) Kinetics of TβRI and TβRII transcript levels in AM after ISS-ODN administration. ISS-ODN was i.v. injected into B6 mice (20 μg/mouse) and the transcription levels of TβRI and II in the isolated AM were analyzed by qPCR. *p < 0.02 in comparison to the 0 hr levels.

The data are shown as the mean ± SD and are representative of two or more experiments.

receptors on AM. As presented in Figure 4E, the inhibition of the TGFβRI and TGFβRII gene expression followed by ISS-ODN administration on AM matched the kinetics of αvβ6 protein expression on AEC (Figure 1B).

Thus, although the regulation of integrin αvβ6 expression by another soluble factor was not ruled out above, we favor a model in which TGFβ associated with AM in their quiescent state most likely control the expression of integrin αvβ6 in AEC. The proposed model of this interaction is presented below.

Actin Polymerization in AM Controls the Expression of Integrin αvβ6 on AEC

In subsequent studies, we analyzed the kinetics of the above observed inhibition of integrin αvβ6. Our initial results demonstrated that the suppression of integrin αvβ6 in vivo started within the first 30 min post-ISS-ODN administration (data not shown). One event that occurs rapidly and is triggered in TLR-activated cells is actin polymerization (Hayashi et al., 2003). Indeed, we observed rapid actin polymerization in AM and in an AM

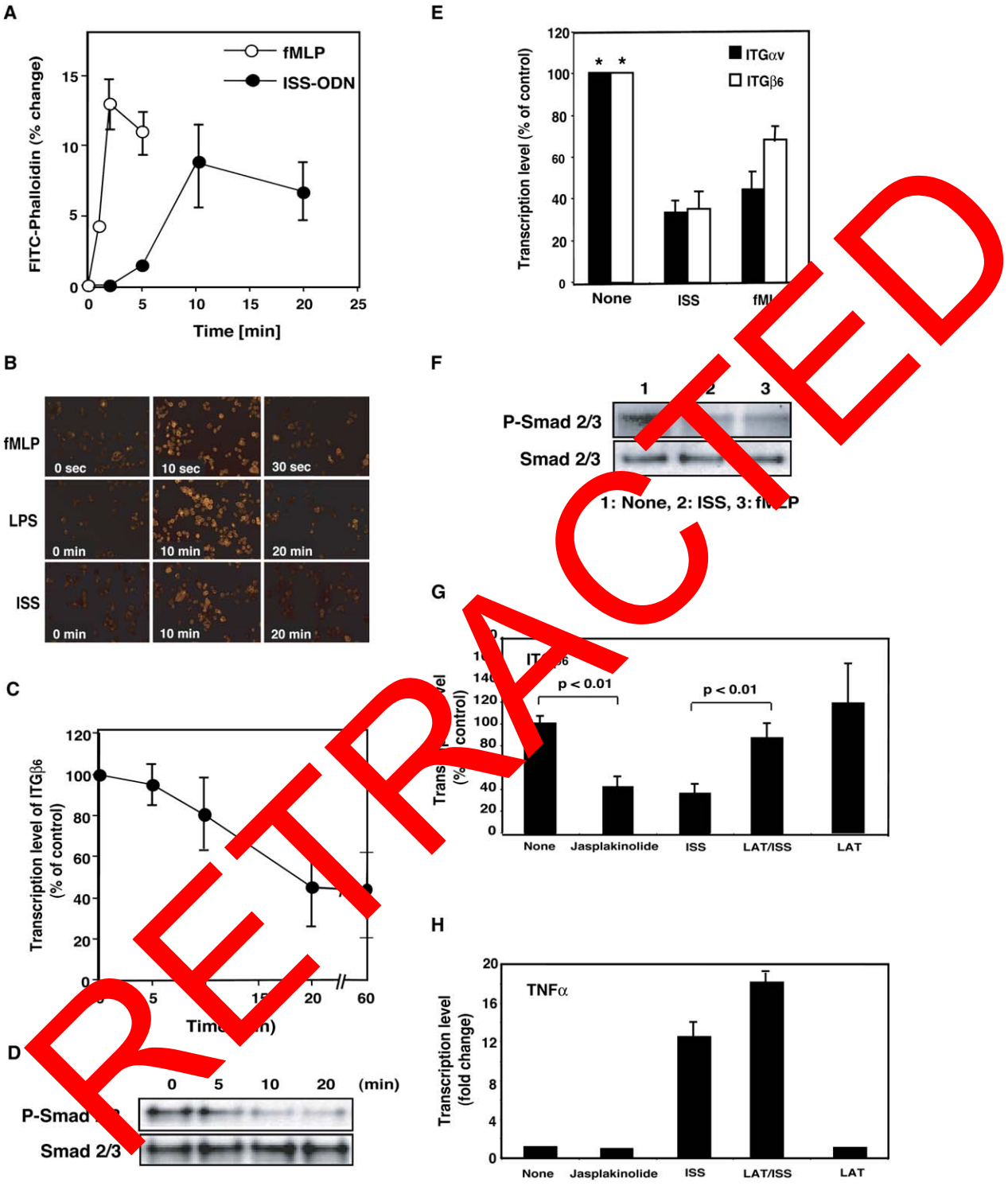

Figure 5. Actin Polymerization in AM Controls the Expression of Integrin αvβ6 on AEC

(A) ISS-ODN induces actin polymerization in AM. AM were isolated from the lung of naive B6 mice and were stimulated with fMLP (10^{-7} M) or ISS-ODN (1 μg/ml) and then stained with FITC-labeled phalloidin, and the fluorescent intensity was measured by FACS (10^5 cells per time point) at the indicated time points.

(B) Microbial products induce actin polymerization in a mAM line (MH-S). MH-S cells were stimulated with LPS, ISS-ODN, and fMLP as above and actin polymerization was determined at appropriate time points by staining with rhodamine-labeled phalloidin followed by visualization under a fluorescent microscope (20× magnification).

(C) Kinetics of integrin β6 transcript levels after ISS-ODN administration. ISS-ODN was i.v. injected into B6 mice (20 μg/mouse), and the levels of integrin β6 in lung tissue were analyzed by qPCR and plotted.

(D) Kinetics of TGFβ signaling after ISS-ODN administration. ISS-ODN was i.v. injected into B6 mice (20 μg/mouse) and the phosphorylation levels of Smad 2/3 in the lung tissue were measured as described above.

cell line (MH-S) stimulated not only with a control stimulator fMLP, but also with TLR4 and TLR9 ligands with a response time of approximately 10 min (Figures 5A and 5B). A minimal response time for the suppression of integrin αvβ6 gene expression by ISS-ODN was once again carefully measured and was shown to start less than 10 min postadministration (Figure 5C). The same time period was identified to inhibit TGFβ signaling in the lung tissue in ISS-ODN-injected mice (Figure 5D). Formyl-MLP (fMLP) is a non-TLR ligand, bacterial peptide that binds to a G protein-coupled receptor (McCoy et al., 1995). Surprisingly, fMLP administration also suppresses the expression of integrin αvβ6 on AEC (Figure 5E) and inhibits subsequent TGFβ signaling in AM (Figure 5F).

The data above suggested that actin polymerization in AM is likely the key event that controls integrin αvβ6 expression on AEC. To address this issue, we evaluated the effects of an inducer and an inhibitor of actin polymerization in our system. Indeed, jasplakinolide (inducer) (O'Reilly et al., 2003) suppressed integrin β6 expression whereas latrunculin-A (inhibitor) (DeFife et al., 1999) reversed the inhibition of this gene induced by ISS-ODN (Figure 5G). As actin polymerization is involved in endocytosis and its inhibition may therefore affect ISS-ODN uptake and consequently the inhibition of TLR9 signaling, we evaluated the induction of ISS-induced TNFα in this system to exclude this possibility. As presented in Figure 5H, TNFα was induced by ISS-ODN in the presence of latrunculin-A, demonstrating that endocytosis was not affected by this compound. Collectively, these results indicate the pivotal role of actin polymerization in AM in the control of integrin αvβ6 expression on AEC.

ISS-Induced MMP9 Restores TGFβ Inhibitory Effects on AM

Our previous data demonstrated that microbial compounds released AM from TGFβ-mediated suppression; however, it was still unclear whether this process is reversible. To explore this issue, we initially checked the kinetics of integrin αvβ6 and the pSmad2/3 levels in the lung tissue after ISS-ODN administration. As shown in Figure 6A, integrin αv expression was profoundly suppressed only in the first 2 days post-ISS-ODN administration. We observed similar kinetics for pSmad2/3 (Figure 6B). As MMPs are involved in the activation of various cytokines and growth factors (Mott and Werb, 2004), we postulated that an ISS-induced MMP could reactivate latent TGFβ. Thus, we initially identified the induction profile of various MMPs in the lung tissue after i.v. ISS-ODN administration. MMP3, MMP8, MMP9, MMP12, and MMP13, but not MMP2, transcripts were induced (Figure 6C). As MMP9 was the only MMP induced within the first 2 days that is also known to activate the latent TGFβ complex (Yu and Stamenkovic, 2000), we hypothesized that this MMP might, therefore, end the cycle of microbial ligand-induced AM activation. To explore the potential role of MMP9 in restoring the TGFβ-mediated suppression on AM, we checked its enzymatic activity (Figure 6D) in the lung tissue after ISS-ODN administration. In preliminary studies, we identified that ISS-induced IFNγ mediates MMP9 expression. Indeed, the administration of ISS-ODN to IFNγ$^{-/-}$ mice failed to induce MMP9 (Figure 6E). Consequently, we observed a prolonged suppression of both integrin β6 levels in the lung tissue (Figure 6E) and TGFβ signaling in AM (Figure 6F) in these mice. To further establish the cause and effect relationship between MMP9 enzymatic activity, TGFβ signaling, and integrin β6 expression, we administrated ISS-ODN in MMP9$^{-/-}$ mice. Indeed, in these mice the kinetics of suppression of integrin β6 expression (Figure 6G) and TGFβ signaling (Figure 6H) were prolonged. Taken together, these data indicate that the subsequent ISS-induced production of MMP9 by AM activates latent TGFβ, reinduces αvβ6 expression on AEC, and thereby reinstates tonic inhibition of AM. The proposed role of this pathway is presented schematically below.

Phagocytic and Bactericidal Activities of AM Post ISS Administration

We demonstrated the transient effects of ISS-ODN on the inhibition of integrin αvβ6 and the phosphorylation levels of Smad2/3 (Figures 6A and 6B). To explore whether the transient release of AM from TGFβ-mediated suppression affects the phagocytic and bactericidal activities of AM, we isolated these cells from mice at different time periods post ISS-ODN injection and measured their responsiveness to subsequent in vitro LPS stimulation. As shown in Figure 7A, AM isolated from mice treated with ISS-ODN for 1 and 2 days prior to in vitro restimulation with LPS produced higher levels of IL-6 and TNFα as compared to AM isolated from naive, nonmanipulated mice (day 0). In contrast, PM isolated from these mice produced very low levels of these cytokines (Figure 7B).

Based on the results displayed in Figure 7A, we isolated AM from mice 1 and 3 days post ISS injection. As predicted, the phagocytic and bactericidal activities of AM isolated 1 day, but not 3 days, post ISS injection were significantly higher upon in vitro infection with *Klebsiella pneumoniae* (Figures 7C and 7D). While PM isolated from the same mice displayed high phagocytic and bactericidal activities, there were no major changes in these activities in PM isolated from mice injected with ISS-ODN either 1 or 3 days prior to bacterial infection in vitro (data not shown).

(E) fMLP suppresses the transcript levels of integrin αv and β6 in lung tissue. fMLP (5 μg/mouse) was i.v. injected into B6 mice. The transcript levels were analyzed by qPCR and compared to those obtained for ISS-ODN (20 μg/mouse). *p < 0.04 compared to noninjected group.
(F) fMLP suppresses the TGFβ signaling in AM. fMLP (5 μg/mouse) was i.v. injected to B6 mice. At 24 hr postinjection, AM were isolated and pSmad 2/3 levels were analyzed and compared to those obtained for ISS-ODN (20 μg/mouse) as described above.
(G) Actin polymerization controls the suppression of integrin β6 gene expression. ISS-ODN (20 μg/mouse), the actin polymerization inducer jasplakinolide (5 μg/mouse), the actin polymerization inhibitor latrunculin-A (20 μg/mouse), or a combination of latrunculin A and ISS-ODN were i.v. injected to B6 mice. The transcript level of ITGβ6 was analyzed by qPCR 2 hr postinjection in lung homogenates.
(H) Latrunculin-A does not block the induction of TNFα by ISS-ODN. The transcript levels of TNFα were measured in the lung homogenates (see above) and analyzed by qPCR.
The data are shown as the mean ± SD and are representative of two or more experiments.

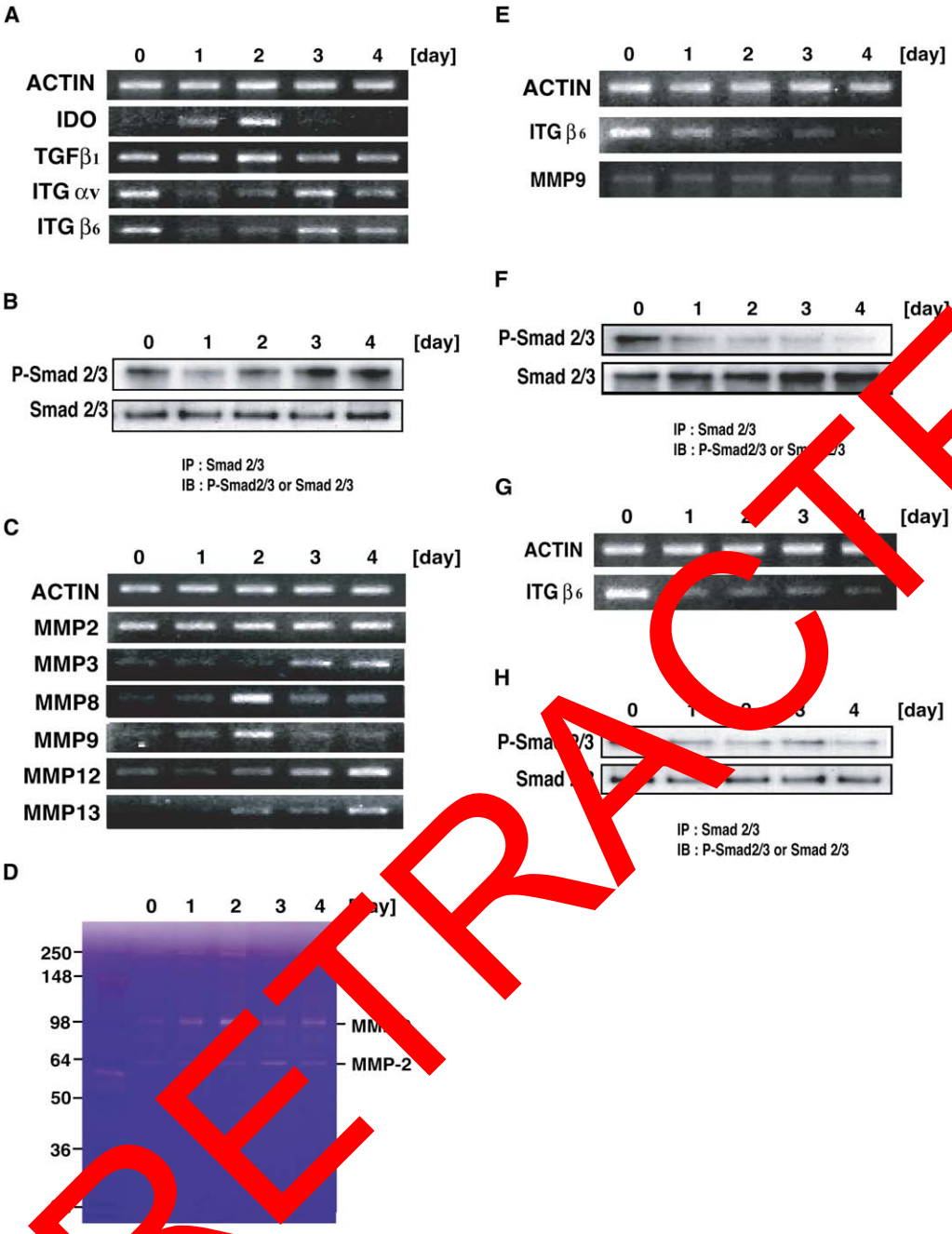

Figure 6. [illegible]duced MMP9 Restores TGFβ Inhibitory Effects on AM

(A) Duration [illegible]he suppression of the transcript levels of integrin αv and β6. B6 mice were i.v. injected with ISS-ODN (20 μg/mouse). The transcript levels of ITGαv [illegible]d β6 and of TGFβ were measured by RT-PCR in lung homogenates. IDO (indolamine 2,3-dioxygenase) transcript levels were used as positive c[illegible]ntrol.

(B) Kinetics of inhibition of TGFβ signaling induced by ISS-ODN. B6 mice were i.v. injected with ISS-ODN (20 μg/mouse), and the pSmad2/3 levels were measured in lung homogenates as described above.

(C) ISS-ODN induces gene transcription of MMPs. B6 mice were i.v. injected with ISS-ODN (20 μg/mouse), and the levels of MMP2, MMP3, MMP8, MMP9, MMP12, and MMP13 were measured by RT-PCR.

(D) ISS-ODN induces MMP9 but not MMP2 gelatinase enzymatic activity. B6 mice were i.v. injected with ISS-ODN, and the enzymatic activity of MMP2 and MMP9 in the lung homogenates was measured by zymography (gelatin gel).

(E) ISS-ODN-induced IFNγ mediates MMP9 transcription. IFNγR$^{-/-}$ mice were i.v. injected with ISS-ODN (20 μg/mouse), and the transcription levels of ITGβ6 and MMP9 were measured in lung homogenates by RT-PCR.

(F) Kinetics of TGFβ signaling in ISS-ODN-injected IFNγR$^{-/-}$ mice. IFNγR$^{-/-}$ mice were i.v. injected with ISS-ODN (20 μg/mouse), and the pSmad2/3 levels were measured in AM homogenates by Western blotting.

(G) In MMP9$^{-/-}$ mice, suppression of ITGβ6 transcript levels by ISS-ODN lasts longer than in wt mice. MMP9$^{-/-}$ mice were i.v. injected with ISS-ODN (20 μg/mouse) and the transcript levels of ITGβ6 was measured by RT-PCR.

(H) In MMP9$^{-/-}$ mice, suppression of TGFβ signaling by ISS-ODN lasts longer than in wt mice. MMP9$^{-/-}$ mice were i.v. injected with ISS-ODN (20 μg/mouse), and the pSmad2/3 levels were measured in AM homogenates by Western blotting.

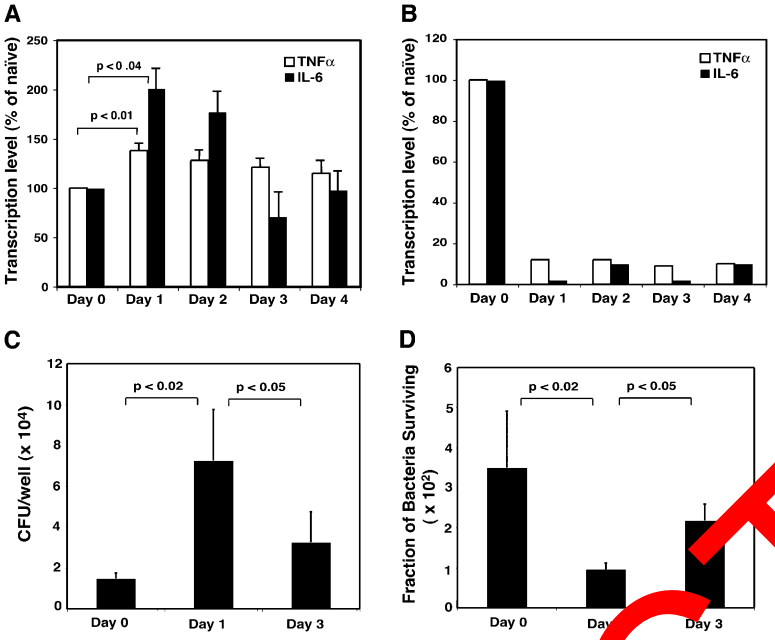

Figure 7. Phagocytic and Bactericidal Activities of AM Post-ISS Administration

(A and B) AM (A) and PM (B) were isolated at different time periods after i.v. ISS-ODN injection (20 μg/mouse) as described. The cells were then stimulated in vitro with LPS (10 ng/ml) for 2 hr. The transcript levels of TNFα and IL-6 were analyzed by qPCR.

(C and D) AM isolated from mice 1 but not 3 days after ISS-ODN injection display enhanced phagocytosis and bactericidal activities upon in vitro infection with *Klebsiella pneumoniae*.

The data are shown as the mean ± SD and are representative of two or more experiments.

Discussion

AM are positioned to sample and respond to inhaled particles and microorganisms that enter the alveolar space. TGFβ, via its unique association with AEC bound integrin αvβ6, inhibits AM functionality under quiescent conditions. In contrast, other factors such as IL-10, PGE2, and IL-10 inhibit AM responses only after these factors have been induced (Bingisser and Holt, 2001). This inhibitory milieu could impede the innate immune response of AM to inhaled microorganisms and consequently make the lung vulnerable to multiple airborne microbial agents unless there is a mechanism that allows a rapid response. Our study provides the mechanisms for this quick and complex adaptation.

The administration of TLR ligands suppressed the basal TGFβ crosstalk between AM-AEC and the subsequent expression of integrin αvβ6 (but not of TGFβ) by AEC. As a result, AM were released from TGFβ-mediated immunosuppression and mounted a higher cytokine response to subsequent TLR stimulation (Figures 2 and 3). The data in Figures 3 and 4 indicate that (1) AM initiate suppression of integrin αvβ6 on nonhematopoietic cells, i.e., AEC, (2) this inhibition is mediated via an AM-AEC, cell-cell interaction, and (3) membrane bound TGFβ is involved in this process.

The rapid inhibition of integrin αvβ6 suggests that the AM-AEC, cell-cell interaction was disrupted (Figure 5). This disruption can be mediated through actin polymerization that modifies the cell shape of TLR-activated AM. Actin polymerization could also lock integrins on the macrophages into an inactive, low-affinity conformation (Kinbara et al., 2003). It also decreases the elasticity of the activated cell (e.g., AM) and consequently interferes with its interactions with neighboring cells (e.g., AEC) (Figure 8B) (Giannone et al., 2004). We confirmed the involvement of actin polymerization in our system by using fMLP and jasplakinolide (inducers of actin polymerization). Both agents activated actin polymerization on AM, which resulted in the inhibition of integrin αvβ6 expression on AEC (Figure 5), whereas latrunculin A (an inhibitor of actin-polymerization) blocked the TLR9-induced inhibition of integrin αvβ6 (Figure 5).

An uncontrolled activation of AM can induce collateral damage in the lung tissue that could lead to organ dysfunction (Morris et al., 2003). Indeed, our data indicate that integrin αvβ6 expression (AEC) and TGFβ signaling (AM) are recovered within 2–3 days poststimulation (Figure 6). We also identified that the administration of TLR9 ligand induced MMP9 transcript and enzymatic activity in the lung via IFNγ secretion (Figure 6). As latent TGFβ is one of the substrates of MMP9, we speculated that MMP9 could turn off AM activation. Indeed, the administration of TLR9 ligand to IFNγR$^{-/-}$ mice resulted in prolonged inhibition of integrin β6 expression (AEC) and TGFβ signaling (AM). Similar results were obtained when TLR9 ligand was injected to MMP9-deficient mice (Figure 6) or coinjected with MMP9 inhibitor to wt mice (data not shown), indicating that TLR-triggered MMP9, through activation of TGFβ, resets this system to its quiescent phase (Figure 8D). Furthermore, the phagocytic and bactericidal activities of AM isolated 1 day, but not 3 days, post ISS-ODN injection were significantly higher upon in vitro infection with *Klebsiella pneumoniae,* confirming the transient nature of AM activation (Figure 7).

Our results illustrate a unique crosstalk between AM and AEC. They describe a novel mechanism that is initiated by different classes of microbial products but with different and distinct signaling pathways (TLR ligands, fMLP) that activate and consequently inactivate innate immunity (i.e., AM) in the alveolar space. We describe this activation-inactivation cycle of innate immunity elicited by microbial products as a homeostatic circuit (Figure 8). The tight control of AM explains how AM can be activated by microbial products or respond to microbial agents in the alveolar space while minimizing their ability to inflict structural injury and functional

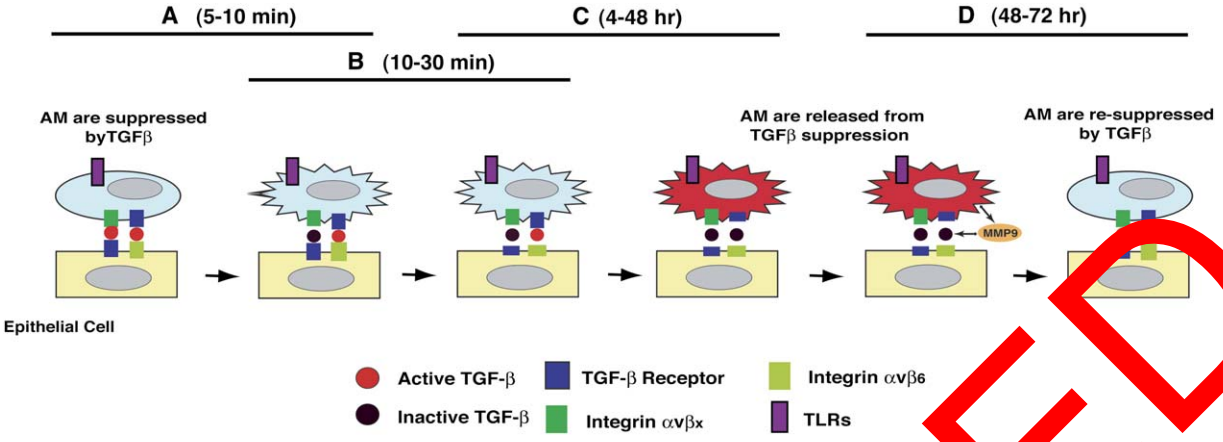

Figure 8. Proposed Scheme of the Homeostatic Circuit

Microbial products activate and inactivate AM through an intricate communication with AEC.

(A) Tonic inhibition of AM by TGFβ presented by integrin αvβ6 on AEC in the steady state. When microbial products enter the subepithelial space, they are recognized by innate immune receptors on AM. This recognition results in a cell shape change in AM due to actin polymerization. Actin polymerization disrupts the TGFβ signaling of AEC initiated by AM (βx = unidentified integrin β-chain) and leads to the disengagement of AM from AEC.

(B) This disengagement impairs the production of TGFβ by AEC and AM and is soon followed by a reduction of TGFβ signaling in both AEC and AM. The basal protein expression of integrin αvβ6 on AEC is no longer maintained. A reduction in the protein levels of integrin αvβ6 on AEC (4–8 hr) results in impaired TGFβ activation of AM.

(C) Subsequent inhibition of TGFβ signaling releases AM from the tonic suppression by TGFβ.

(D) After 48 hr, AM produce MMP9 that activates latent TGFβ. The active TGFβ then binds to its receptor on both AM and AEC, reinduces integrin αvβ6 and αvβx expression, and subsequently reinstates the tonic inhibition of AM observed in the steady state.

damage to the adjacent lung tissue. Furthermore, these results underscore the concept of organ-specific innate immunity and propose that in addition to the unique biochemical characteristics of a variety of signature microbial products (e.g., TLR ligands), tissue-specific microenvironmental factors are also involved in shaping organ-specific defense strategies against microbial invasion. Finally, on a practical level, our data provide the insight to expand the activation phase of innate immunity in the lung, a process that can be utilized to reduce the risk of illness due to any airborne microbial agent (Figure 7), including those that can be used for bioterrorism purposes.

Experimental Procedures

Reagents

We used the following abs: monoclonal anti-mouse integrin αvβ6 (10D5), anti-mouse integrin αv for Western blotting (Chemicon, Temecula, CA), anti-mouse integrin αv chain (anti-mouse CD51, BD Pharmingen, San Diego, CA), and anti-TGFβ1-3 (1D11, R&D Systems, Inc., Minneapolis, MN) for blocking in cocultures, anti-Smad2/3 (Santa Cruz Biotechnology, Santa Cruz, CA), and anti-phospho Smad2/3 (Cell Signaling Technology, Beverly, MA). The sources of TLR ligands were mentioned elsewhere (Hayashi et al., 2003). Flagellin was kindly provided by Dr. J.A. Didonato (Cleveland Clinic Foundation, Cleveland, OH). fMLP, Jasplakinolide, and Latrunculin were purchased from Calbiochem (San Diego, CA). Recombinant active TGFβ1 was purchased from PeproTech, Inc (Rocky Hill, NJ). The mouse pulmonary epithelial cell lines, MLE12 and MLE15, and mouse AM cell line, MH-S, were purchased from American Type Culture Collection (Rockville, MD). Mouse TGFβ ELISA was performed with a DuoSet ELISA kit purchased from R&D Systems.

Mice

Female C57Bl/6 (B6) wild-type mice, 5–6 weeks of age, and cytokine-deficient mice, i.e., IFNγ$^{-/-}$, IL-12p40$^{-/-}$ IL-10$^{-/-}$, COX2$^{-/-}$, and TLR2/4$^{-/-}$ (B6), were purchased from The Jackson Laboratory (Bar Harbor, ME). IFNα/βR$^{-/-}$ mice (129) were purchased from UK Universal (East Yorkshire, UK). TLR9-deficient (B6) mice were obtained from Dr. S. Akira (Osaka University, Osaka, Japan) and bred at the University of California, San Diego (San Diego, CA). Human (h) ITGβ6 transgenic mice (B6) were generated and bred at the University of California, San Francisco (Huang et al., 1998). MMP9 mice and their wild-type controls (FVB) were purchase from The Jackson Laboratory.

Generation and Validation of Bone Marrow Chimeric Mice

TLR9$^{-/-}$/wt chimeric mice were generated as described (Cho et al., 2002). On the day of transfer, the recipient mice received whole body irradiation with 1000 rad from a 137 Cs source at the Irradiation Facility, UCSD. Bone marrow cells were harvested from the femurs of the donor mice (TLR9$^{-/-}$ or wt mice) and resuspended in RPMI-1640 media without FCS, and 10 × 10^6 bone marrow cells were i.v. injected into irradiated recipient mice. Four groups of chimeras were created: wt to wt, wt to TLR9$^{-/-}$, TLR9$^{-/-}$ to wt, and TLR9$^{-/-}$ to TLR9$^{-/-}$. The recipient mice were continued on antibiotics for 6 weeks after bone marrow transfer to minimize the risk of inadvertent infections. 6 weeks after transfer, the recipient mice were screened for % of chimerism by qPCR. Primers used for wt allele are 5′-AGG AAG GTT CTG GGC TCA AT-3′ and 5′-TCT GTA CCC CGT TTC TCT GC-3′ that yield a 200 bp product. Primers used for KO allele are 5′-TCT GTA CCC CGT TTC TCT GC-3′ and 5′-ATC GCC TTC TAT CGC CTT CTT GAC GAG-3′ that yield a 220 bp product. A standard curve was created via blood mixtures of wt and TLR9$^{-/-}$ mice in various ratios. The percentage of wt or TLR9$^{-/-}$ DNA in the chimeras was then calculated by this standard curve. Mice demonstrating >90% chimerisms were used in experiments.

Transfer of Primary Isolated AM after Depletion of Resident AM in Donor Mice

AM depletion in mice was achieved by intranasal (i.n.) administration of a total of 120 μl of a liposome-encapsulated clodronate suspension (Vrije Universiteit, Amsterdam, The Netherlands). Under light anesthesia, 40 μl of liposomes was i.n. delivered to TLR9$^{-/-}$ mice, three times in 1 day, 2 hr apart. This procedure depleted ~70%–90% of resident AM as determined by total macrophage counts

identified by morphology in the bronchoalveolar lavage fluid 48 hr after liposome delivery. AM for transfer were prepared from either wt (C57BL/6) or TLR9$^{-/-}$ donor mice by bronchoalveolar lavage by means of cold PBS containing 1 mM EDTA. 2 × 10^6 wt or TLR9$^{-/-}$ AM were delivered intratracheally to the lungs of TLR9$^{-/-}$ recipient mice that had received clodronate liposomes 48 hr previously.

Infection of Alveolar Macrophages with *Klebsiella pneumoniae* In Vitro

Alveolar macrophages were harvested by bronchoalveolar lavage, resuspended in RPMI supplemented with 10% fetal bovine serum, seeded into 48-well plates at a density of 3 × 10^5 cells/well, and allowed to adhere for 90 min at 37ºC in a 5% CO_2 incubator. Assays of bacterial phagocytosis and intracellular survival were modified from previously described procedures (Browne et al., 2002; Libby et al., 2000). The inoculum consisted of *Klebsiella pneumoniae* ATCC strain 43816 (Deng et al., 2004), grown to stationary phase in LB medium (Chen et al., 1995). The bacteria were diluted 1:5 (vol/vol) with LB, washed once with Dulbecco's phosphate-buffered saline (DPBS), resuspended in DPBS, mixed 1:1 (vol/vol) with fresh heparinized mouse plasma, and incubated at 37ºC for 20 min. The opsonized bacteria were diluted in DPBS and used to inoculate the macrophage cultures at a ratio of 20 bacteria per macrophage. The infected cultures were centrifuged at 200 × g for 5 min to bring the bacteria in contact with the macrophages, then incubated 45 min at 37ºC. The medium was removed and replaced with fresh RPMI containing 10% fetal bovine serum and gentamicin at 20 μg/ml to kill extracellular bacteria. The initial number of intracellular bacteria (phagocytosis assay) was determined by incubation for an additional 45 min at 37ºC, removal of the culture media, lysis of macrophages by the addition of 0.5% deoxycholate in DPBS, and detection of bacterial colony-forming units (CFU) by serial dilution and plating on LB agar. Intracellular survival was determined by incubation of infected cultures for 24 hr after addition of the gentamicin medium, followed by harvest and detection of CFU as described above. Survival was expressed as the CFU remaining after 24 hr/initial CFU after phagocytosis.

Semiquantitative RT-PCR and Real-Time RT-PCR

Total RNA was prepared from tissue from cultured cells by means of TRIzol reagent according to the manufacturer's instructions (Invitrogen, Carlsbad, CA). Total RNA (3–5 μg) was subjected to reverse transcription with the SuperScript II Reverse Transcriptase and reaction conditions specified by the manufacturer (Invitrogen). The transcript of target genes was then determined with a semiquantitative one-step RT-PCR with β-actin as an internal control. PCR was carried out under the following conditions: 94ºC, 1 min; 68ºC, 2 min for each cycle, and the PCR products were separated on a 1.4% agarose gel and visualized by ethidium bromide staining. Expression of target genes was normalized to that of β-actin. The RT-PCR primers specific for target genes were designed based on the reported sequences, using the Primer 3 program (primer3_www.v 0.1 β) and synthesized by IDT Technologies (Caralville, IA). Primer sequences can be found in the Supplemental Data available on this article online. For quantitation of the transcription level of target genes, RNA samples were further analyzed by real-time PCR with TaqMan Universal PCR Master Mix (Applied Biosystems, Foster City, CA).

Immunoprecipitation

Immunoprecipitation was performed by standard methodologies. Lung tissue or AM were homogenized in lysis buffer (10 mM HEPES [pH 7.9], 10 mM KCl, 0.1 mM EDTA, 0.1 mM EGTA, 1% Triton X-100, 1 mM glycerophosphate, 2.5 mM sodium pyrophosphate, 1 mM sodium orthovanadate) containing protease inhibitor cocktails (Sigma). 100 μg of each of lung crude extract was mixed with primary antibody (2 μg/ml) and incubated at 4ºC with constant mixing for 12 hr. For immunoprecipitation of integrin αvβ6 and Smad 2/3, the samples were mixed with mouse monoclonal antibody against integrin αvβ6 (10D5) (Chemicon) and with goat polyclonal antibody against Smad 2/3 (Santa Cruz Biotechnology), respectively. The immunocomplex was captured by the addition of packed protein A crosslinked 4% beaded agarose (Calbiochem) (50 μl/500 μl supernatant) for 2 hr at 4ºC. Beads were washed three times with lysis buffer. Samples were subsequently subjected to immunoblot/Western analysis as described below.

Immunoblot/Western Analysis

Beads with immunocomplexes were resuspended in loading buffer, heated at 95ºC for 3 min, and elecrophoresed on 10%–20% Tricine SDS-PAGE (Invitrogen). After electrophoresis, the proteins were transferred onto PVDF membrane in a buffer containing 25 mM Tris-Hcl (pH 8.3)/192 mM glycine/20% methanol and blocked with TBST (50 mM Tris-HCl [pH 7.5]/150 mM NaCl/0.1% Tween 20) containing 2% of bovine serum albumin for at least 1 hr. The blots were washed three times with TBST and then incubated overnight with primary antibody. For detection of integrin αvβ6 and phosphorylated Smad 2/3, the blots were incubated with rabbit polyclonal antibodies against integrin αv (Chemicon) or against phospho-Smad 2/3 (Cell Signaling Technology), respectively. The blots were subsequently washed three times with TBST and incubated with horseradish peroxidase-conjugated anti-rabbit IgG secondary antibody (Pierce). Proteins were visualized by ECL detection system (Amersham Biosciences) according to the manufacturer's instruction.

In Vitro Stimulation of AM with ISS

Primary AM were obtained from naive or from ISS-ODN (20 μg/mouse)-treated C57BL/6 mice (24 hr postadministration) by bronchoalveolar lavage (BAL) using sterile PBS containing 1 mM EDTA. AM were plated in 24-well plate at 1 × 10^5 cells/well in final volume of 1 ml RPMI-1640 medium (BioWhittaker, Walkersville, MD) supplemented with 10% heat-inactivated fetal bovine serum. When indicated, cells were stimulated with LPS (10 ng/ml) for 2 hr.

ISS-Induced Conditioned Media

Conditioned media were prepared from a single-cell suspension of lung tissue or spleen of C57BL/6 mice that were stimulated with 10 μg/ml ISS-ODN for 48 hr. Conditioned media from unstimulated lung cells or spleen cells were used as a control. C57BL/6 mice or TLR9$^{-/-}$ mice (nonresponsive to ISS-ODN) were intraperitoneally (i.p.) injected with 1 ml of ISS-conditioned media or control media and then sacrificed 24 hr postinjection. Lungs were harvested and analyzed for transcription level of integrin αvβ6.

In Vitro Bi- or Coculture of AM with Epithelial Cells

MLE12 cells (AEC) were grown in HITES medium (RPMI-1640 supplemented with insulin, transferrin, sodium selenite [Sigma, St. Louis, MO], 10 mM hydrocortisone [Sigma], 10 mM β-estradiol [Sigma], HEPES [Sigma], penicillin/streptomycin [Sigma], and 2% heat-inactivated fetal calf serum) in 24- or 48-well plates until confluent. AM were isolated by BAL from B6 mice.

In some experiments, a portion of primary isolated AM were pretreated with 10 μg/ml anti-TGFβ ab (R&D Systems) for 1 hr at 37ºC. 10 μg/ml of this antibody is reported by the manufacturer to neutralize up to 25 ng TGFβ/ml. Without washing out the antibody in order to neutralize any further TGFβ secreted by AEC, 0.6 × 10^5 AM were added to wells containing confluent AEC (= coculture). In some experiments, a portion of freshly isolated AM were pretreated with 20 μg/ml anti-integrin αv ab (BD Pharmingen) for 1 hr at 37ºC. The AM were then washed twice to remove the antibody before adding to wells containing AEC.

Other experiments used AM added to wells either with (= biculture) or without (= coculture) a transwell insert (0.4 μM, Corning, Inc., Corning, NY), which physically separated the AM from coming into direct contact with AEC. All co- and biculture experiments were then incubated overnight at 37ºC (24 hr).

Detection of MMP2 and MMP9 by Zymography

Proteolytic activity of MMP-2 and MMP-9 was analyzed by zymography as described (Martinez-Torres et al., 2004). Lung tissue crude extracts in loading buffer were loaded on 10% polyacrylamide gels (Invitrogen) containing 0.1% gelatin. After electrophoresis, the gels were incubated in 50 mM Tris-HCl (pH 7.5) containing 0.2 M NaCl, 5 mM $CaCl_2$, and 2.5% Triton X-100 for 30–60 min and subsequently incubated overnight at room temperature in the same buffer without Triton X-100. The gels were then stained with Coomassie blue (0.25% Coomassie blue, 10% methanol, and 10% glacial acetic acid) and destained in the same solution without dye.

Measurement of F-Actin Polymerization in Macrophages

F-actin content in macrophages activated by LPS or ISS-ODN was assessed by flow cytometry (Kutsuna et al., 2004) or by fluorescent microscopy.

For flow cytometry experiments, AM (B6) or the murine cell line MH-S (ATCC) were stimulated with ISS-ODN (final 1 μg/ml) or LPS (final 10 ng/ml) for 5, 10, or 20 min in polypropylene tubes. The cells were then fixed, permeabilized, and stained with FITC-phalloidin in a single step with the addition of a solution of formaldehyde and saponin (Fix/Perm, BD Pharmingen) containing 5 ng/ml FITC-phalliodin (Sigma) for 15 min at room temperature in the dark. The cells were washed with PBS containing saponin and subjected to flow cytometry.

For fluorescent microscopy experiments, AM (MH-S cell line) were seeded onto chamber slides overnight. ISS-ODN (1 μg/ml), LPS (10 ng/ml), fMLP (10^{-7} M), or media were added for various times, and the cells were fixed and permeabilized before the addition of rhodamine-labeled phalloidin for 15 min at room temperature. The slides were washed and coverslips added before being examined microscopically.

Statistical Analysis

Data are expressed as mean ± standard deviation. Statistical analysis was performed according to the Student's t test for unpaired data. $p < 0.05$ was considered significant.

Supplemental Data

Supplemental Experimental Procedures can be found with this article online at http://www.immunity.com/cgi/content/full/24/4/475/DC1/.

Acknowledgments

This work is supported by NIH grants AI40682, AI57709, AI56453, and HL79449 (E.R.) and HL56365, HL64353, HL53949, and HL66600 (D.S.).

Received: April 20, 2005
Revised: December 28, 2005
Accepted: February 1, 2006
Published: April 18, 2006

References

Annes, J.P., Munger, J.S., and Ri[illegible], D.B. [illegible]03). Making sen[illegible] of latent TGFbeta activation. J. Cell Sci. *116*, 217[illegible]24.

Bingisser, R.M., and Holt, [illegible]. (2001). Immunom[illegible]ulating mechanisms in the lower respi[illegible]ory tract: nitric oxide me[illegible]ted interactions between alveol[illegible]macropha[illegible], epithelial cells, and T-cells. Swiss Med. Wkly. *13*[illegible]171–179.

Browne, S.H., Lesnick, [illegible]d Guiney, [illegible]. (2002). Genetic requirements f[illegible]*onella*-[illegible]uced cyto[illegible]nology in human monocyte-deri[illegible] macr[illegible]nages. I[illegible]t. Im[illegible]n. *70*, 7126–7135.

Chen[illegible]., Buchm[illegible]er, N.A., Lib[illegible]., Fang, F.C., Krause, M., and Gui[illegible]D.G. (199[illegible]Central regulatory role for the RpoS sigma factor in [illegible]ress[illegible] of Sal[illegible]a dublin plasmid virulence genes. J. Bacter[illegible]*7*, 5303–5309.

Cho, H.J., Ha[illegible]hi, T., Datta, S.K., Takabayashi, K., Van Uden, J.H., Horner, A., Co[illegible]., and Raz, E. (2002). IFN-alpha beta promote priming of antigen specific CD8+ and CD4+ T lymphocytes by immunostimulatory DNA-based vaccines. J. Immunol. *168*, 4907–4913.

DeFife, K.M., Jenney, C.R., Colton, E., and Anderson, J.M. (1999). Disruption of filamentous actin inhibits human macrophage fusion. FASEB J. *13*, 823–832.

Deng, J.C., Moore, T.A., Newstead, M.W., Zeng, X., Krieg, A.M., and Standiford, T.J. (2004). CpG oligodeoxynucleotides stimulate protective innate immunity against pulmonary *Klebsiella* infection. J. Immunol. *173*, 5148–5155.

Dobrovolskaia, M.A., Medvedev, A.E., Thomas, K.E., Cuesta, N., Toshchakov, V., Ren, T., Cody, M.J., Michalek, S.M., Rice, N.R., and Vogel, S.N. (2003). Induction of in vitro reprogramming by Toll-like receptor (TLR)2 and TLR4 agonists in murine macrophages: effects of TLR "homotolerance" versus "heterotolerance" on NF-kappa B signaling pathway components. J. Immunol. *170*, 508–519.

Fitzpatrick, D.R., and Bielefeldt-Ohmann, H. (1999). Transforming growth factor beta in infectious disease: always there for the host and the pathogen. Trends Microbiol. *7*, 232–236.

Giannone, G., Dubin-Thaler, B.J., Dobereiner, H.G., Kieffer, N., Bresnick, A.R., and Sheetz, M.P. (2004). Periodic lamellipodial contractions correlate with rearward actin waves. Cell *116*, 431–443.

Hayashi, F., Means, T.K., and Luster, A.D. (2003). Toll-like re[illegible]ptors stimulate human neutrophil function. Blood *102*, 2660[illegible]9.

Huang, X., Wu, J., Zhu, W., Pytela, R., and Sher[illegible]rd, D. (1998). Expression of the human integrin beta6 subuni[illegible]alveolar type II cells and bronchiolar epithelial cells reverses lung [illegible]flammation in beta6 knockout mice. Am. J. Respir. Cell M[illegible]. Biol. *19*[illegible]636–642.

Hynes, R.O. (2002). Integrins: bidirecti[illegible]al, allosteric sig[illegible]g ma[illegible]chines. Cell *110*, 673–687.

Kinbara, K., Goldfinger, L.E., Hans[illegible]M., Cho[illegible].L., and Ginsberg, M.H. (2003). Ras GTPases: int[illegible]rins [illegible]nd[illegible] foes? Nat[illegible]v. Mol. Cell Biol. *4*, 767–776.

Krutzik, S.R., and Modl[illegible]L. (2004). The r[illegible]f To[illegible]like receptors in combating mycob[illegible]teria[illegible]min. Immunol. [illegible]5–41.

Kutsuna, H., Suzuki, K., Kama[illegible]N., Kato, T., Hato, F., Mizuno, K., Kobayashi, H., Ishii, M., and Kitag[illegible]a, S. (2004). Actin reorganization and m[illegible]gical changes in[illegible]man neutrophils stimulated by TNF, [illegible]l-CSF, and G-CSF: the role of MAP kinases. Am. J. Physiol. Cel[illegible]ysiol. *286*, C55–C64.

Libby, [illegible]., Lesnick, M., [illegible]segawa, P., Weidenhammer, E., and Guiney, [illegible]G. (2000). The *S[illegible]monella* virulence plasmid spv genes are requir[illegible]or cytopath[illegible]gy in human monocyte-derived macrophages. Cell[illegible]*2*, 49–58.

Li[illegible]ab, M.F., Pollard, A.M., and Yates, J.L. (1993). A role for TGF-b[illegible]he suppression by murine bronchoalveolar cells of lun[illegible]endritic[illegible]ell initiated immune responses. Reg. Immunol. *5*, [illegible]–157.

[illegible]rtinez-Torres, F.J., Wagner, S., Haas, J., Kehm, R., Sellner, J., H[illegible]ke, W., and Meyding-Lamade, U. (2004). Increased presence of matrix metalloproteinases 2 and 9 in short- and long-term experimental herpes simplex virus encephalitis. Neurosci. Lett. *368*, 274–278.

McCoy, R., Haviland, D.L., Molmenti, E.P., Ziambaras, T., Wetsel, R.A., and Perlmutter, D.H. (1995). N-formylpeptide and complement C5a receptors are expressed in liver cells and mediate hepatic acute phase gene regulation. J. Exp. Med. *182*, 207–217.

Morris, D.G., Huang, X., Kaminski, N., Wang, Y., Shapiro, S.D., Dolganov, G., Glick, A., and Sheppard, D. (2003). Loss of integrin alpha(v)beta6-mediated TGF-beta activation causes Mmp12-dependent emphysema. Nature *422*, 169–173.

Mott, J.D., and Werb, Z. (2004). Regulation of matrix biology by matrix metalloproteinases. Curr. Opin. Cell Biol. *16*, 558–564.

Munger, J.S., Huang, X., Kawakatsu, H., Griffiths, M.J., Dalton, S.L., Wu, J., Pittet, J.F., Kaminski, N., Garat, C., Matthay, M.A., et al. (1999). The integrin alpha v beta 6 binds and activates latent TGF beta 1: a mechanism for regulating pulmonary inflammation and fibrosis. Cell *96*, 319–328.

O'Reilly, P.J., Hickman-Davis, J.M., Davis, I.C., and Matalon, S. (2003). Hyperoxia impairs antibacterial function of macrophages through effects on actin. Am. J. Respir. Cell Mol. Biol. *28*, 443–450.

Shi, Y., and Massague, J. (2003). Mechanisms of TGF-beta signaling from cell membrane to the nucleus. Cell *113*, 685–700.

Takeda, K., Kaisho, T., and Akira, S. (2003). Toll-like receptors. Annu. Rev. Immunol. *21*, 335–376.

Thepen, T., Kraal, G., and Holt, P.G. (1994). The role of alveolar macrophages in regulation of lung inflammation. Ann. N Y Acad. Sci. *725*, 200–206.

van der Flier, A., and Sonnenberg, A. (2001). Function and interactions of integrins. Cell Tissue Res. *305*, 285–298.

Yu, Q., and Stamenkovic, I. (2000). Cell surface-localized matrix metalloproteinase-9 proteolytically activates TGF-beta and promotes tumor invasion and angiogenesis. Genes Dev. *14*, 163–176.

Zambruno, G., Marchisio, P.C., Marconi, A., Vaschieri, C., Melchiori, A., Giannetti, A., and De Luca, M. (1995). Transforming growth factor-beta 1 modulates beta 1 and beta 5 integrin receptors and induces the de novo expression of the alpha v beta 6 heterodimer in normal human keratinocytes: implications for wound healing. J. Cell Biol. *129*, 853–865.